Published OnlineFirst December 14, 2010; DOI:10.1158/1541-7786.MCR-10-0340

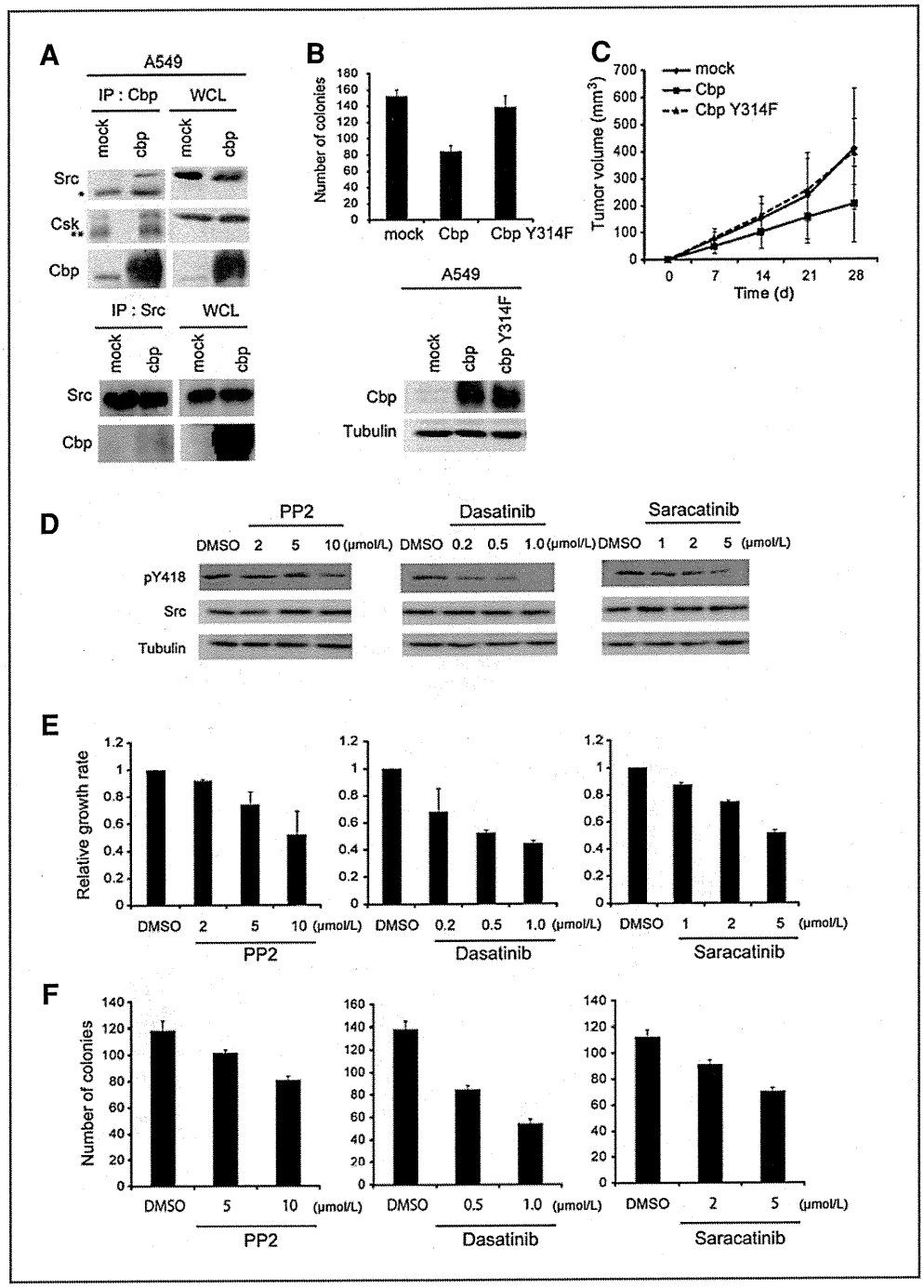

Figure 4. Cbp-Csk association and inhibition of c-Src are involved in the growth suppression of A549 cells. A, cell lysates from mock and Cbp-expressing A549 cells were immunoprecipitated with anti-Cbp antibody, and the immunoprecipitates were analyzed by Western blotting with anti-Src, anti-Csk, or anti-Cbp antibody. To detect Csk in the immunoprecipitates, the sample was not heat denatured so as to avoid an overlap with the IgG heavy chain on the gel. *, the location of the IgG heavy chain; **, the non-specific bands. B, the anchorage-independent growth of mock cells, Cbp-expressing cells, and Cbp mutant-expressing cells (Cbp Y314F) were examined by a colony formation assay in soft agar. Colonies were stained with MTT 14 days after plating. The colony numbers per cm^2 ± SE that were obtained from 3 independent experiments are shown (left). The expression levels of Cbp wild type and Cbp mutants were assessed by Western blotting. C, the ability of tumor formation was compared in mouse xenograft models. The tumor volumes (mean ± SE) that were obtained from 4 mice are plotted as a function of days after inoculation. D, A549 cells were incubated with increasing concentrations of PP2, Dasatinib, Saracatinib or DMSO for 24 hours, and the total cell lysates were subjected to Western blotting with the indicated antibodies. E, *in vitro* proliferation assays were performed for A549 cells incubated with the indicated Src inhibitor. The relative growth rate (mean ± SE) was obtained from 3 independent experiments. F, colony formation assays were performed for A549 cells incubated with DMSO, PP2, Dasatinib, or Saracatinib at the concentrations indicated. Colonies were stained with MTT 10 days after plating. The colony numbers per cm^2 (mean ± SE) were obtained from 3 independent experiments. Student's *t* tests: *, $P < 0.05$.

Published OnlineFirst December 14, 2010; DOI:10.1158/1541-7786.MCR-10-0340

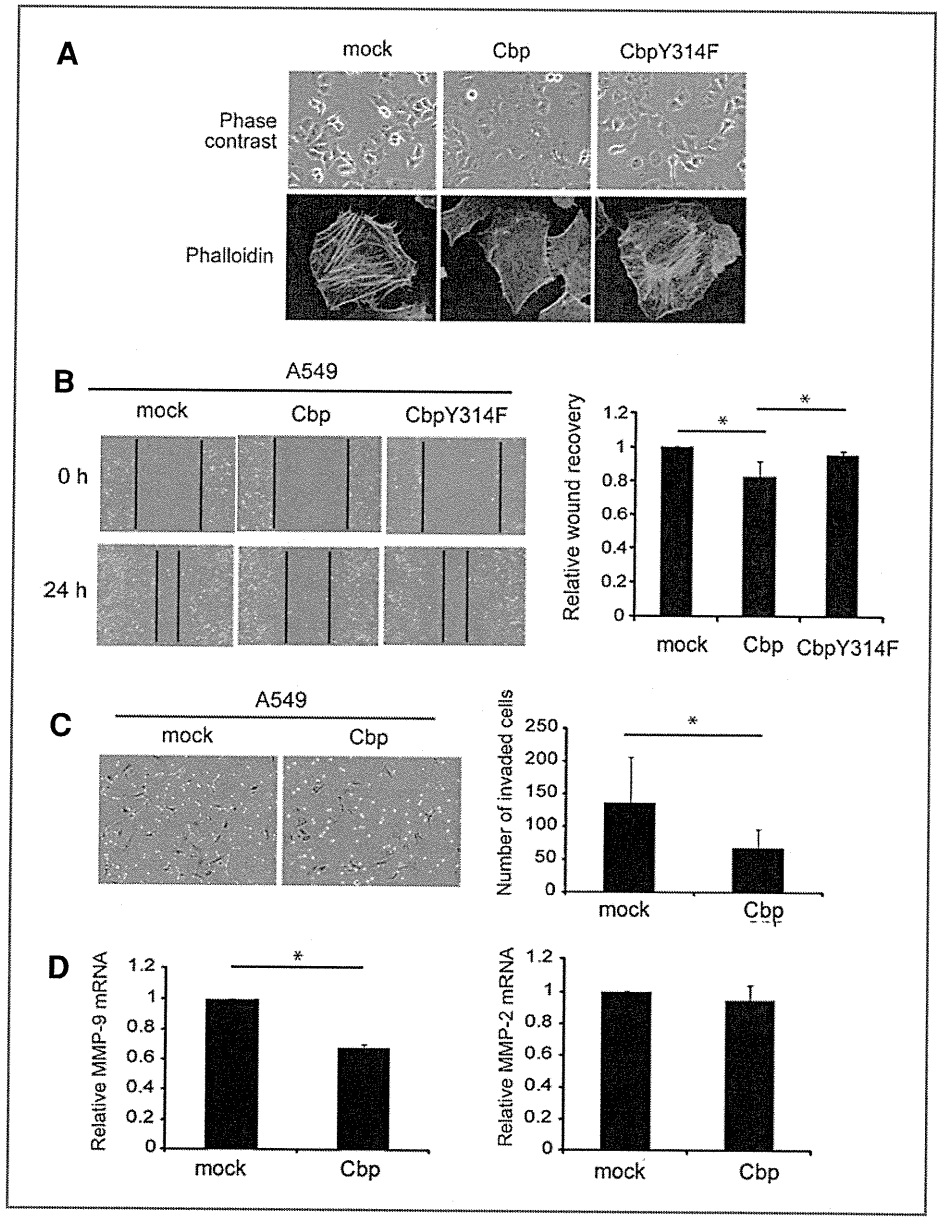

Figure 5. The impact of Cbp expression on cytoskeletal organization and the motility of lung cancer cells. A, actin stress fibers were stained with Alexa Fluor 488 phalloidin. B, the wound-healing analysis was conducted. The wounded areas were photographed at 0 and 24 hours after the monolayer cultures were scratched (left). The gaps of the wound areas were measured, and the relative values (mean ± SE) from triplicate experiments are shown (right); *, $P < 0.05$. C, invasion assays were carried out in Matrigel transwell chambers. After incubation for 24 hours, the cells that had passed through the filter into the bottom wells were fixed and photographed (left). The cells in the bottom wells were counted, and the mean ± SE from 3 independent experiments is shown (right). D, the expression of MMP-9 and MMP-2 was analyzed by quantitative real-time PCR. Data represent the relative values (mean ± SE); *, $P < 0.05$.

A549 cells, with or without Cbp expression, were intravenously injected into nude mice, and the pulmonary metastatic burden was assessed by counting the number of tumor nodules on the surface of the lung. Mice in the control groups displayed numerous distinguishable pulmonary nodules, whereas mice that were injected with Cbp-expressing cells exhibited fewer visible nodules (Fig. 6A).

To examine whether the levels of Cbp expression in lung cancer affected the degree of tumor progression, the expression of Cbp mRNA was examined in primary lung adenocarcinoma by quantitative PCR using total RNA from FFPE tissue samples as templates. The lowest score of Cbp mRNA in 12 cases was arbitrarily set as 1.0, and the relative level of Cbp mRNA in each cancer specimen was evaluated. As shown in Figure 6B, appreciable differences in the levels of Cbp mRNA were observed among individual samples, although there was no significant relationship between the Cbp expression levels and the histologic tumor grade; however, Cbp expression could be significantly correlated with lymph node involvement. The mean Cbp score for tumors without lymph node metastases was 7.71 ± 4.38, whereas the mean Cbp score for tumors with lymph node metastases was 3.20 ± 2.05 (Fig. 6C). These findings suggest that the level of Cbp in lung cancer may be correlated with metastatic potential to the lymph node rather than primary tumor grade.

Published OnlineFirst December 14, 2010; DOI:10.1158/1541-7786.MCR-10-0340

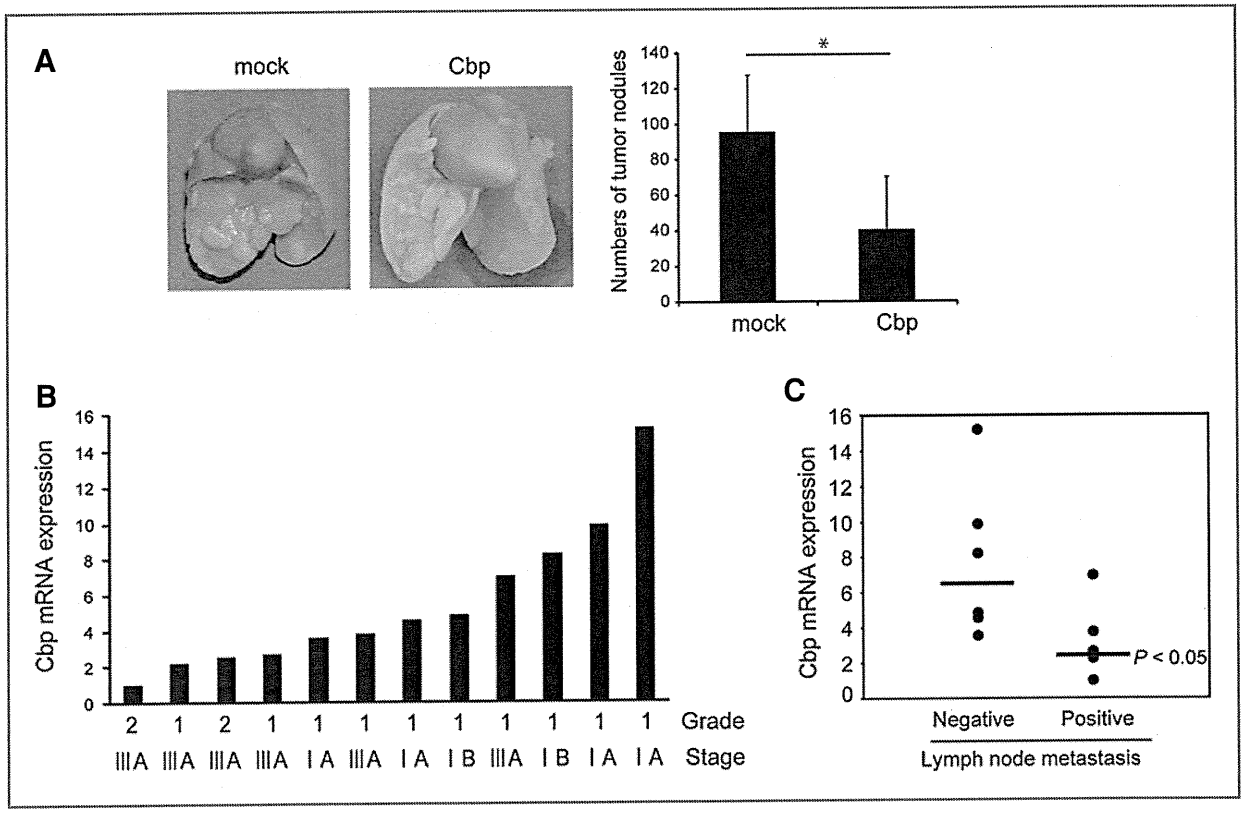

Figure 6. The expression of Cbp inhibits metastasis of lung cancer cells. A, mock or Cbp-expressing A549 cells were injected into the tail veins of nude mice as described in the Materials and Methods section. Pulmonary metastatic burden was assessed by counting the number of tumor nodules on the lung surface (left). The mean values ± SE from 5 mice are shown (right). B, quantitative real-time PCR was performed using total RNA that was isolated from FFPE tissue samples. The relative levels of Cbp mRNA, which were normalized to GAPDH mRNA expression, from the primary cancer specimens of each case were compared. Pathologic stages and tumor grades (1: well-differentiated and 2: moderately or poorly differentiated) are indicated at the bottom. C, the levels of Cbp mRNA in cases with lymph node metastases were compared with those of cases without metastases. The bar indicates the mean value of the Cbp level; ANOVA: *, $P < 0.05$.

Discussion

In this study, we found that the expression of Cbp is significantly downregulated in various human NSCLC cell lines and tissues. Due to its role as a scaffold for both active c-Src and Csk, Cbp expression was observed to suppress the tumor growth of A549 and Lu99 cells, which have substantially upregulated c-Src. In addition, we have shown that the expression of Cbp suppresses cell motility, *in vitro* invasiveness, and the *in vivo* metastatic potential of A549 cells, and the expression level of Cbp was significantly correlated with lymph node involvement in human lung cancers. These findings suggest the important role of Cbp in controlling the malignant potential of NSCLC, particularly those that have upregulated c-Src activities.

Recently, several studies have implicated a role for Cbp in tumor malignancy. Cbp may function as a negative regulator of EGF-induced cell transformation (26). In colon cancer cells, Cbp is downregulated and the introduction of Cbp suppresses tumorigenesis (19). In this study, we have shown that Cbp acts as a suppressor of NSCLC tumor progression by controlling c-Src signaling. On the other hand, it has been reported that the expression of Cbp is increased in a significant majority of diffuse large B-cell lymphomas (27). In RCC, Cbp is overexpressed in cancer tissues and enhances cell motility and invasiveness, wherein it regulates RhoA activity via its PDZ-binding domain (20). These observations suggest that Cbp has distinct functions depending on the cancer type. To elucidate the molecular basis for the distinct functions of Cbp, a more extensive analysis of Cbp function in each case will be necessary.

In the immune system, lipid rafts have been thought to play a positive role in signaling that is initiated through the T-cell, B-cell, and Fc receptors (28, 29). In contrast, we previously proposed a role for Cbp in suppressing c-Src–mediated transformation using a model system (19). In this study, we provide firm evidence that Cbp in lipid rafts plays a suppressive role in controlling the c-Src–induced malignant potential of human cancer cells. Biochemical analysis demonstrated that Cbp recruits active c-Src and Csk into

Published OnlineFirst December 14, 2010; DOI:10.1158/1541-7786.MCR-10-0340

lipid rafts by forming a Cbp–Csk–c-Src complex and serves as a scaffold where the efficient inactivation of c-Src by Csk can be achieved. As a consequence, active c-Src is eliminated from the non–raft compartments, and this elimination potentially contributes to the suppression of the non–raft FAK that is crucial for tumor growth. These findings indicate that the function of c-Src may be regulated not only on the activity level but also by influencing the intracellular distribution that is determined by the specific scaffold Cbp. In contrast to the overexpression of Cbp, the overexpression of Csk failed to suppress the tumor growth of A549 cells (data not shown). This intriguing result further supports the requirement of Cbp in Csk-mediated c-Src regulation as well as in the control of malignancy of A549 cells.

Recent reports have shown that c-Src is altered and highly activated in NSCLC, especially in adenocarcinomas (7, 9, 30). The level of c-Src kinase activity has been reported to correlate with tumor size in NSCLC (8). Furthermore, the mitogenic effect of both nicotine and asbestos in NSCLC cells is likely to involve the activation of c-Src (31, 32). These observations suggest that c-Src activity is frequently associated with the malignant progression of a variety of NSCLC cells. Because c-Src is also known to be an important mediator of upregulated receptor tyrosine kinases, including HER2 and EGFR, therapeutic strategies to inhibit c-Src activity are currently being developed (33). Recently, several inhibitors of activated c-Src in cancer cells have been examined in clinical trials for the treatment of not only lung but also breast, colon, and prostate cancer (34). In preclinical studies, NSCLC cells that were treated with dasatinib (BMS-354825) demonstrated decreased cell growth and changes in downstream signaling that resulted in a reduced capability for invasion (35, 36). These reports suggest that c-Src could be an attractive target for treatment in a particular subset of patients with NSCLC. Therefore, the c-Src regulatory circuit that consists of Csk, Cbp, and lipid rafts may offer new targets that can prevent the progression of NSCLC by controlling c-Src function.

In addition to tumor growth, the *in vivo* invasiveness of A549 cells was also significantly inhibited by the overexpression of Cbp. The attenuation of actin stress fiber formation and the downregulation of MMP-9 expression may explain the lower invasiveness of Cbp-expressing cells. This result was consistent with the previous observation that c-Src activation promoted tumor invasiveness (25). Recently, it has been demonstrated that Src-FAK signaling through JNK (c-jun NH kinase) alters the transcriptional regulation of MMP-9 (37), and that the pharmacologic blockade of Src activity suppresses VEGF-induced MMP production in squamous carcinoma cells (38). These lines of evidence support that the inhibition of c-Src and FAK functions through the overexpression of Cbp leads to the modulation of cytoskeletal organization and MMP production. We have also found that the expression levels of Cbp mRNA that were detected in FFPE NSCLC samples (39) in cases with lymph node involvement were lower than those in cases without lymph node involvement. This raises the possibility that the level of Cbp in primary tumors is generally relevant to the metastatic potential of NSCLC; however, the molecular mechanism by which the expression of Cbp is specifically downregulated in NSCLC remains to be addressed. Because there was no apparent correlation between c-Src upregulation and Cbp downregulation, pathways other than c-Src signaling may also contribute to Cbp downregulation mechanisms. The elucidation of the pathway(s) that lead to Cbp downregulation may shed light on the mechanisms of tumor progression and offer potential new opportunities for therapeutic intervention in NSCLC.

Disclosure of Potential Conflicts of Interest

No potential conflicts of interest were disclosed.

Acknowledgment

We thank Drs. T. Akagi, K. Kodama, and M. Yutsudo for their generous gifts of reagents.

Grant Support

The Ministry of Education, Culture, Sports, Science, and Technology of Japan (grants-in-aid for Scientific Research) and the Uehara Memorial Foundation.

The costs of publication of this article were defrayed in part by the payment of page charges. This article must therefore be hereby marked *advertisement* in accordance with 18 U.S.C. Section 1734 solely to indicate this fact.

Received July 27, 2010; revised November 29, 2010; accepted December 2, 2010; published OnlineFirst December 14, 2010.

References

1. Yang L, Fujimoto J, Qiu D, Sakamoto N. Trends in cancer mortality in the elderly in Japan, 1970–2007. Ann Oncol 2010;21:389–96.
2. Risch A, Plass C. Lung cancer epigenetics and genetics. Int J Cancer 2008;123:1–7.
3. Miller VA, Kris MG, Shah N, Patel J, Azzoli C, Gomez J, et al. Bronchioloalveolar pathologic subtype and smoking history predict sensitivity to gefitinib in advanced non-small-cell lung cancer. J Clin Oncol 2004;22:1103–9.
4. Jove R, Hanafusa H. Cell transformation by the viral src oncogene. Annu Rev Cell Biol 1987;3:31–56.
5. Brown MT, Cooper JA. Regulation, substrates and functions of src. Biochim Biophys Acta 1996;1287:121–49.
6. Biscardi JS, Tice DA, Parsons SJ. c-Src, receptor tyrosine kinases, and human cancer. Adv Cancer Res 1999;76:61–119.
7. Mazurenko NN, Kogan EA, Zborovskaya IB, Kisseljov FL. Expression of pp60c-src in human small cell and non-small cell lung carcinomas. Eur J Cancer 1992;28:372–7.
8. Masaki T, Igarashi K, Tokuda M, Yukimasa S, Han F, Jin YJ, et al. pp60c-src activation in lung adenocarcinoma. Eur J Cancer 2003; 39:1447–55.
9. Frame MC. Src in cancer: deregulation and consequences for cell behaviour. Biochim Biophys Acta 2002;1602:114–30.
10. Frame MC. Newest findings on the oldest oncogene; how activated src does it. J Cell Sci 2004;117:989–98.

Published OnlineFirst December 14, 2010; DOI:10.1158/1541-7786.MCR-10-0340

11. Tan YX, Wang HT, Zhang P, Yan ZH, Dai GL, Wu MC, et al. c-src activating mutation analysis in Chinese patients with colorectal cancer. World J Gastroenterol 2005;11:2351–3.
12. Nada S, Okada M, MacAuley A, Cooper JA, Nakagawa H. Cloning of a complementary DNA for a protein-tyrosine kinase that specifically phosphorylates a negative regulatory site of p60c-src. Nature 1991; 351:69–72.
13. Nada S, Yagi T, Takeda H, Tokunaga T, Nakagawa H, Ikawa Y, et al. Constitutive activation of Src family kinases in mouse embryos that lack Csk. Cell 1993;73:1125–35.
14. Masaki T, Okada M, Tokuda M, Shiratori Y, Hatase O, Shirai M, et al. Reduced C-terminal Src kinase (Csk) activities in hepatocellular carcinoma. Hepatology 1999;29:379–84.
15. Okada M, Nada S, Yamanashi Y, Yamamoto T, Nakagawa H. CSK: a protein-tyrosine kinase involved in regulation of src family kinases. J Biol Chem 1991;266:24249–52.
16. Brdicka T, Pavlistova D, Leo A, Bruyns E, Korinek V, Angelisova P, et al. Phosphoprotein associated with glycosphingolipid-enriched microdomains (PAG), a novel ubiquitously expressed transmembrane adaptor protein, binds the protein tyrosine kinase csk and is involved in regulation of T cell activation. J Exp Med 2000;191: 1591–604.
17. Kawabuchi M, Satomi Y, Takao T, Shimonishi Y, Nada S, Nagai K, et al. Transmembrane phosphoprotein Cbp regulates the activities of Src-family tyrosine kinases. Nature 2000;404:999–1003.
18. Oneyama C, Iino T, Saito K, Suzuki K, Ogawa A, Okada M. Transforming potential of Src family kinases is limited by the cholesterol-enriched membrane microdomain. Mol Cell Biol 2009;29:6462–72.
19. Oneyama C, Hikita T, Enya K, Dobenecker MW, Saito K, Nada S, et al. The lipid raft-anchored adaptor protein Cbp controls the oncogenic potential of c-Src. Mol Cell 2008; 30:426–36.
20. Feng X, Lu X, Man X, Zhou W, Jiang LQ, Knyazev P, et al. Overexpression of Csk-binding protein contributes to renal cell carcinogenesis. Oncogene 2009;28:3320–31.
21. Akagi T, Sasai K, Hanafusa H. Refractory nature of normal human diploid fibroblasts with respect to oncogene-mediated transformation. Proc Natl Acad Sci USA 2003;100:13567–72.
22. Zhu Q, Krakowski AR, Dunham EE, Wang L, Bandyopadhyay A, Berdeaux R, et al. Dual role of SnoN in mammalian tumorigenesis. Mol Cell Biol 2007;27:324–39.
23. Shima T, Nada S, Okada M. Transmembrane phosphoprotein Cbp senses cell adhesion signaling mediated by Src family kinase in lipid rafts. Proc Natl Acad Sci USA 2003;100:14897–902.
24. Lichtenberg D, Goni FM, Heerklotz H. Detergent-resistant membranes should not be identified with membrane rafts. Trends Biochem Sci 2005;30:430–6.
25. Irby RB, Yeatman TJ. Role of Src expression and activation in human cancer. Oncogene 2000;19:5636–42.
26. Jiang LQ, Feng X, Zhou W, Knyazev PG, Ullrich A, Chen Z. Csk-binding protein (Cbp) negatively regulates epidermal growth factor-induced cell transformation by controlling Src activation. Oncogene 2006;25: 5495–506.
27. Svec A. Expression of transmembrane adaptor protein PAG/Cbp in diffuse large B-cell lymphoma: immunohistochemical study of 73 cases. Pathol Res Pract 2007;203:193–8.
28. Horejsi V. Lipid rafts and their roles in T-cell activation. Microbes Infect 2005;7:310–6.
29. Resh MD. The ups and downs of SRC regulation: tumor suppression by Cbp. Cancer Cell 2008;13:469–71.
30. Budde RJ, Ke S, Levin VA. Activity of pp60c-src in 60 different cell lines derived from human tumors. Cancer Biochem Biophys 1994;14:171–5.
31. Dasgupta P, Rastogi S, Pillai S, Ordonez-Ercan D, Morris M, Haura E, et al. Nicotine induces cell proliferation by beta-arrestin-mediated activation of Src and Rb-Raf-1 pathways. J Clin Invest 2006; 116:2208–17.
32. Scapoli L, Ramos-Nino ME, Martinelli M, Mossman BT. Src-dependent ERK5 and Src/EGFR-dependent ERK1/2 activation is required for cell proliferation by asbestos. Oncogene 2004;23:805–13.
33. Knowlden JM, Hutcheson IR, Jones HE, Madden T, Gee JM, Harper ME, et al. Elevated levels of epidermal growth factor receptor/c-erbB2 heterodimers mediate an autocrine growth regulatory pathway in tamoxifen-resistant MCF-7 cells. Endocrinology 2003;144:1032–44.
34. Kim LC, Song L, Haura EB. Src kinases as therapeutic targets for cancer. Nat Rev Clin Oncol 2009;6:587–95.
35. Song L, Morris M, Bagui T, Lee FY, Jove R, Haura EB. Dasatinib (BMS-354825) selectively induces apoptosis in lung cancer cells dependent on epidermal growth factor receptor signaling for survival. Cancer Res 2006;66:5542–8.
36. Johnson FM, Saigal B, Talpaz M, Donato NJ. Dasatinib (BMS-354825) tyrosine kinase inhibitor suppresses invasion and induces cell cycle arrest and apoptosis of head and neck squamous cell carcinoma and non-small cell lung cancer cells. Clin Cancer Res 2005;11:6924–32.
37. Hsia DA, Mitra SK, Hauck CR, Streblow DN, Nelson JA, Ilic D, et al. Differential regulation of cell motility and invasion by FAK. J Cell Biol 2003;160:753–67.
38. Donnini S, Monti M, Castagnini C, Solito R, Botta M, Schenone S, et al. Pyrazolo-pyrimidine-derived c-Src inhibitor reduces angiogenesis and survival of squamous carcinoma cells by suppressing vascular endothelial growth factor production and signaling. Int J Cancer 2007;120:995–1004.
39. Cronin M, Pho M, Dutta D, Stephans JC, Shak S, Kiefer MC, et al. Measurement of gene expression in archival paraffin-embedded tissues: development and performance of a 92-gene reverse transcriptase-polymerase chain reaction assay. Am J Pathol 2004; 164:35–42.

Epithelial to Mesenchymal Transition Is a Determinant of Sensitivity to Chemoradiotherapy in Non-Small Cell Lung Cancer

Yasushi Shintani, MD, PhD, Akira Okimura, DDS, PhD, Katsutoshi Sato, PhD, Tomoyuki Nakagiri, MD, PhD, Yoshihisa Kadota, MD, PhD, Masayohi Inoue, MD, PhD, Noriyoshi Sawabata, MD, PhD, Masato Minami, MD, PhD, Naoki Ikeda, MD, PhD, Kunimistu Kawahara, MD, PhD, Tomoshige Matsumoto, MD, PhD, Nariaki Matsuura, MD, PhD, Mitsunori Ohta, MD, PhD, and Meinoshin Okumura, MD, PhD

Department of General Thoracic Surgery, Osaka University Graduate School of Medicine, Osaka; Departments of General Thoracic Surgery, Pathology, and Clinical Research, and Development, Osaka Prefectural Medical Center for Respiratory and Allergic Disease, Osaka; and Department of Molecular Pathology, Graduate School of Medicine and Health Sciences, Osaka University, Suita, Osaka, Japan

Background. The epithelial to mesenchymal transition (EMT) is a fundamental biological process during which epithelial cells change to a mesenchymal phenotype; it has a profound impact on cancer progression. The purpose of this study was to clarify the role of EMT in the sensitivity of non-small cell lung cancer (NSCLC) to chemoradiotherapy (CRT).

Methods. We evaluated the correlation between EMT and sensitivity to chemotherapy or radiotherapy using NSCLC cells induced to undergo EMT with epidermal growth factor or transforming growth factor-β1. Immunohistochemistry was used to examine the expression of EMT markers, E-cadherin, cytokeratin, N-cadherin, and vimentin in 50 tumor specimens obtained from patients with NSCLC both before and after CRT.

Results. The EMT resulted in increased malignant potential and reduced sensitivity to cisplatin and paclitaxel in NSCLC cells. Furthermore, chronic exposure to cisplatin, paclitaxel, or radiation altered the cells into therapy-resistant sub-lines that showed phenotypic changes such as a spindle-cell shape and increased EMT marker expression. Also, decreased expression of epithelial markers and upregulation of mesenchymal markers were detected in surgically resected specimens after CRT compared with biopsy specimens obtained before treatment. The disease-free survival rate of patients with EMT marker-positive tumors was significantly lower than that of those with EMT marker-negative tumors.

Conclusions. The EMT marker expression was detected in NSCLC tumors after CRT, indicating that EMT changes are associated with insensitivity to CRT. New therapeutic combinations using EMT-signaling inhibitors may be needed to circumvent the resistance of some types of cancer to CRT.

(Ann Thorac Surg 2011;92:1794–1804)

The results of surgical resection alone for locally advanced non-small cell lung cancer (NSCLC) are poor, and thus the option of induction chemoradiotherapy (CRT) has been developed [1–3]. Although there is consensus about the indication for a multimodal approach in most patients with locally advanced disease, there is no clear agreement about which local therapy should be applied in any given situation [4]. Another continuing problem in the management of lung cancer is metastatic disease, which indicates the importance of gaining a better understanding of biological changes that promote the aggressive neoplastic phenotype [5].

The epithelial to mesenchymal transition (EMT) is a fundamental biological process during which epithelial cells lose their polarity and change to a mesenchymal phenotype [6]. Hallmarks of EMT include loss of cell-cell adhesion, reorganization of the actin cytoskeleton, and acquisition of increased migratory characteristics [7]. When cancer cells invade adjacent tissues or metastasize, they use a mechanism similar to EMT [8]. E-cadherin is a transmembrane glycoprotein that mediates cell-cell adhesion and maintains the normal polarized epithelial phenotype, and functions as a tumor suppressor [9, 10]. Many studies have shown that expression of an inappropriate mesenchymal cadherin in epithelial cells is another means by which tumor cells alter their adhesive function [11, 12]. Thus it has been proposed that increased expressions of EMT markers,

Accepted for publication July 15, 2011.

Presented at the Forty-seventh Annual Meeting of The Society of Thoracic Surgeons, San Diego, CA, Jan 31–Feb 2, 2011.

Address correspondence to Dr Shintani, Department of General Thoracic Surgery, Osaka University Graduate School of Medicine, 2-2-L5 Yamadaoka, Suita-city, Osaka 565-0871, Japan; e-mail: yshintani@thoracic.med.osaka-u.ac.jp.

0003-4975/$36.00
doi:10.1016/j.athoracsur.2011.07.032

loss of epithelial markers such as E-cadherin and cytokeratin, and altered expressions of mesenchymal markers such as N-cadherin and vimentin are associated with poor prognosis in NSCLC cases [13–15].

A few recent studies have reported roles for EMT in the chemoresistance of cancer cells to anti-NSCLC agents [16–18]. Some investigators have reported that the EMT process is resistant to apoptosis [19]. Autocrine production of transforming growth factor-beta (TGF-β) confers resistance to apoptosis after an epithelial-mesenchymal transition process in hepatocytes; the role of EGF receptor ligands. We previously reported that the EMT process increases survival signaling through a phosphatidylinositol 3′-kinase to extracellular signal-regulated kinases pathway [20]. Thus we hypothesized that EMT might alter NSCLC tumors and make them insensitive to chemoradiotherapy. To identify new targets for prevention of metastasis, it is important to understand the molecular mechanisms that drive EMT. In the present study, we evaluated the correlation between EMT and sensitivity to chemotherapy or radiotherapy using epidermal growth factor (EGF) or TGF-β1 to induce EMT in NSCLC cells. In addition, we investigated whether EMT was related to acquired resistance to clinical CRT treatment by evaluating tissue samples obtained from patients with NSCLC before and after CRT.

Material and Methods

Reagents, Antibodies, and Cultured Cells

The A549 cells were purchased from American Type Culture Collection (ATCC, Manassas, VA) and maintained in RPMI (Roswell Park Memorial Institute) medium with 10% fetal bovine serum. Antibodies and other reagents used in this study are shown in Appendix 1. Immunofluorescence microscopy and trans-well motility assays were performed as previously described [12].

Real-Time Polymerase Chain Reaction (RT-PCR)

Real-time PCR using TaqMan assays (Applied Biosystems, Carlsbad, CA) was performed using a CFX96 system (BioRad, Hercules, CA). Threshold cycle (Ct) values were determined from triplicate reactions for the test and reference samples of each target and the internal control gene (GAPDH [glyceraldehyde-3-phosphate dehydrogenase]). Relative expression levels were calculated as 2-ΔΔCt.

Cell Viability and Clonogenic Assay

The MTT assays were used to assess cell viability according to the manufacturer's protocol (Roche Applied Science, Mannheim, Germany). Each experiment was performed using 6 replicate wells and 3 independent experiments. The IC_{50} was defined as the drug concentration required to produce a 50% reduction of the optimal density in each test. For the clonogenic assay, 1,000 cells were plated at equal density in 100-mm culture dishes and cultured with or without the indicated reagents for 14 days. The cells were stained with 0.25% crystal violet for 5 minutes and the number of colonies was counted manually. All experiments were performed in triplicate.

Establishment of Treatment-Resistant Cell Lines

Treatment-resistant cell lines were generated from parental cells by continuous exposure to the drugs according to the methods described by Bertolini and colleagues [21]. Briefly, cells were exposed to 30-μM cisplatin or 2-μM paclitaxel in RPMI media, and surviving cells were continuously exposed to increasing dosages and maintained in the culture media at concentrations of 60 μM and 5 μM. To create a radiation-resistant cell line, A549 cells were treated with radiation at 2 Gy per week for a total dose of 60 Gy. A 4-MV X-ray device, obtained from the linear accelerator at Osaka University Graduate School of Medicine, was used to deliver a dose rate of 1.8 Gy per minute. Some cell sub-lines were cloned using a limited dilution method and resistance to radiation was confirmed by further radiation treatment.

Study Population

Sixty-three patients underwent preoperative concurrent CRT and pulmonary resection between 1995 and 2005 at the Osaka Prefectural Medical Center for Respiratory and Allergic Disease, and Osaka University Hospital. An Institutional Review Board approved this retrospective study and written informed consent for surgical intervention was obtained from each patient. Each patient received 2 cycles of cisplatin-vinca alkaloid or cisplatindocetaxel-based chemotherapy every 4 weeks: cisplatin at 80 mg/m^2 on day 1, and vindesine at 3 mg/m^2 on days 1 and 8, with or without mitomycin at 8 mg/m^2 on day 1 [PV(M) regimen]; cisplatin at 80 mg/m^2 on day 1 and vinorelbine at 20 mg/m^2 on days 1 and 8 (nPV regimen); cisplatin at 80 mg/m^2 on day 1 and docetaxel at 60 mg/m^2 on day 1 (DP regimen). Radiotherapy directed at the tumor and mediastinal nodes was started on day 2 at doses greater than 40 Gy and was performed concurrently during cycle 1. A thoracotomy was performed 6 to 8 weeks after completion of CRT and all patients were performed complete resections.

Immunohistochemistry

A primary antibody reaction was performed using antibodies listed in Appendix 1, then incubated overnight at 4°C. The EnVision+ anti-mouse/HRP polymer (DAKO, Carpinteria, CA) was applied and peroxidase activity was visualized with a diaminobenzidine tetrahydrochloride solution. The slides were examined separately by 2 independent pathologists (A.O. and K.K.) unaware of the clinical characteristics of the patients. All sections were scored in a semiquantitative manner according to the modified method described previously by McCarty and colleagues [22] which reflects both the intensity and percentage of cells. Intensity (I) was classified as 0 (no staining), +1 (weak staining), +2 (distinct staining), or +3 (very strong staining). Tumor cells were counted in three ×200 fields and the per-

Ann Thorac Surg
2011;92:1794–1804

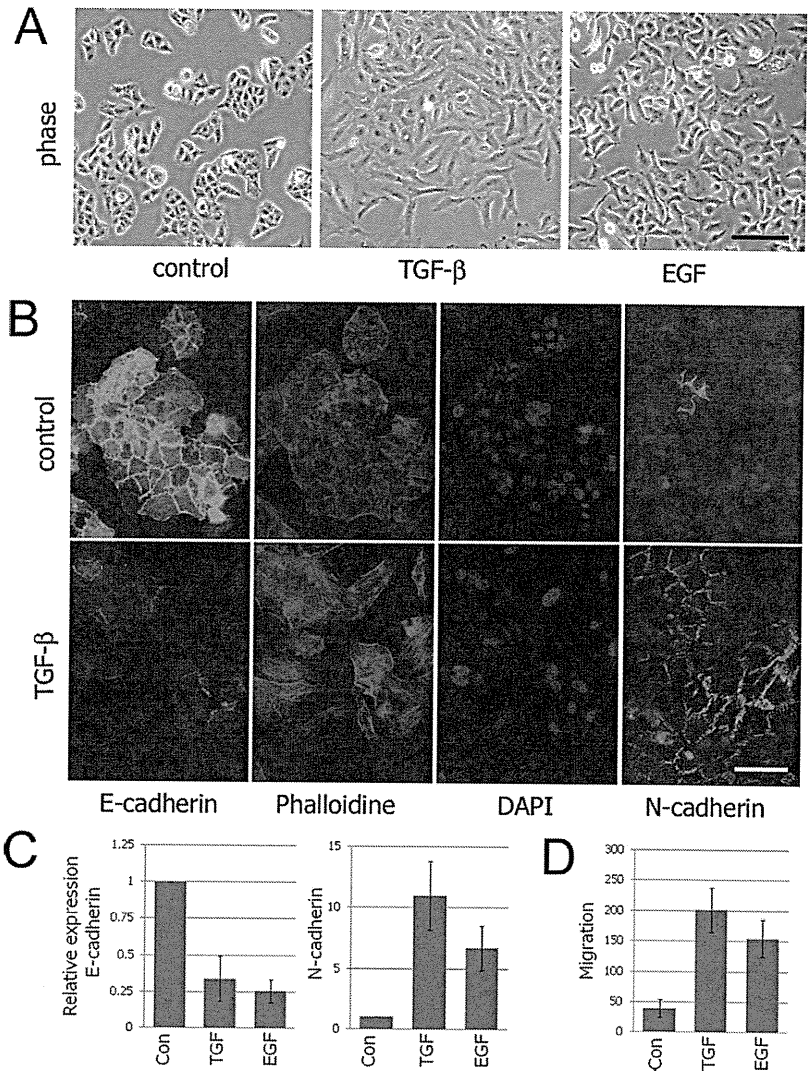

Fig 1. (A) The A549 cells were treated with PBS (as a control), TGF-β1 (2 ng/mL), and EGF (100 ng/mL) for 2 days. Phase contrast images were obtained using a 4.2× objective lens. Bar = 100 μm. (B) The A549 cells were stained for E-cadherin, N-cadherin, 4′,6-diamidino-2-phenylindole, and phalloidine after treatment with PBS (as a control) or TGF-β1 (2 ng/mL). Photographs were obtained using a 40× objective lens. Bar = 50 μm. (C) A549 cells were treated with PBS (control), TGF-β1 (2 ng/mL), or EGF (100 ng/mL) for 1 day, RT-PCR performed to detect E-cadherin and N-cadherin. (D) Motility assays were performed and cells traversing the filter were counted. Columns represent mean values, and bars the standard deviation ($p < 0.05$; control versus TGF or EGF). (con = control; EGF = epidermal growth factor; PBS = phosphate buffered saline; RT-PCR = real-time polymerase chain reaction; TGF = transforming growth factor.)

centage of carcinoma cells with positive staining for each marker was scored. The staining score was calculated for each slide by using the following algorithm: Staining grade (SG) = Σ (I × percentage of carcinoma cells) and the SG was classified as 0 (score<10), +1 (10≤, <30), +2 (30≤, <70), or +3 (70≤).

Statistical Design and Data Analysis

A χ^2 test or Mann-Whitney *U* test was used to compare the results. The disease-free survival (DFS) rates were compared with the results of a log-rank test. The DFS was defined as the time between the date of pulmonary resection and the date of recurrent disease. All patient characteristics were tested against DFS using a Cox-regression analysis based on the tested variable. All statistical analyses were performed using Statview version 5.0 for Windows (Abacus Concepts, Berkeley, CA). A *p* value of less than 0.05 was considered to be statistically significant.

Results

EMT-Induced NSCLC Cells Resistant to Treatment

The TGF-β and EGF both induced EMT in A549 cells, which became more scattered and spindle shaped (Fig 1A). The immunofluorescence (IF) and RT-PCR analysis showed that the expression of E-cadherin decreased, while that of N-cadherin and vimentin increased in EMT-induced cells (Fig 1B, C). In addition, our migration assay findings showed an increased number of cells after EMT induction (Fig 1D), indicating increased malignancy potential.

To determine whether EMT induction resulted in reduced sensitivity to chemotherapy agents such as cisplatin and paclitaxel, we treated the cells with various concentrations of these agents for 2 days after inducing EMT with TGF-β or EGF. The EMT-induced cells showed a significant increase in cell viability in response to cisplatin or paclitaxel compared with untreated control

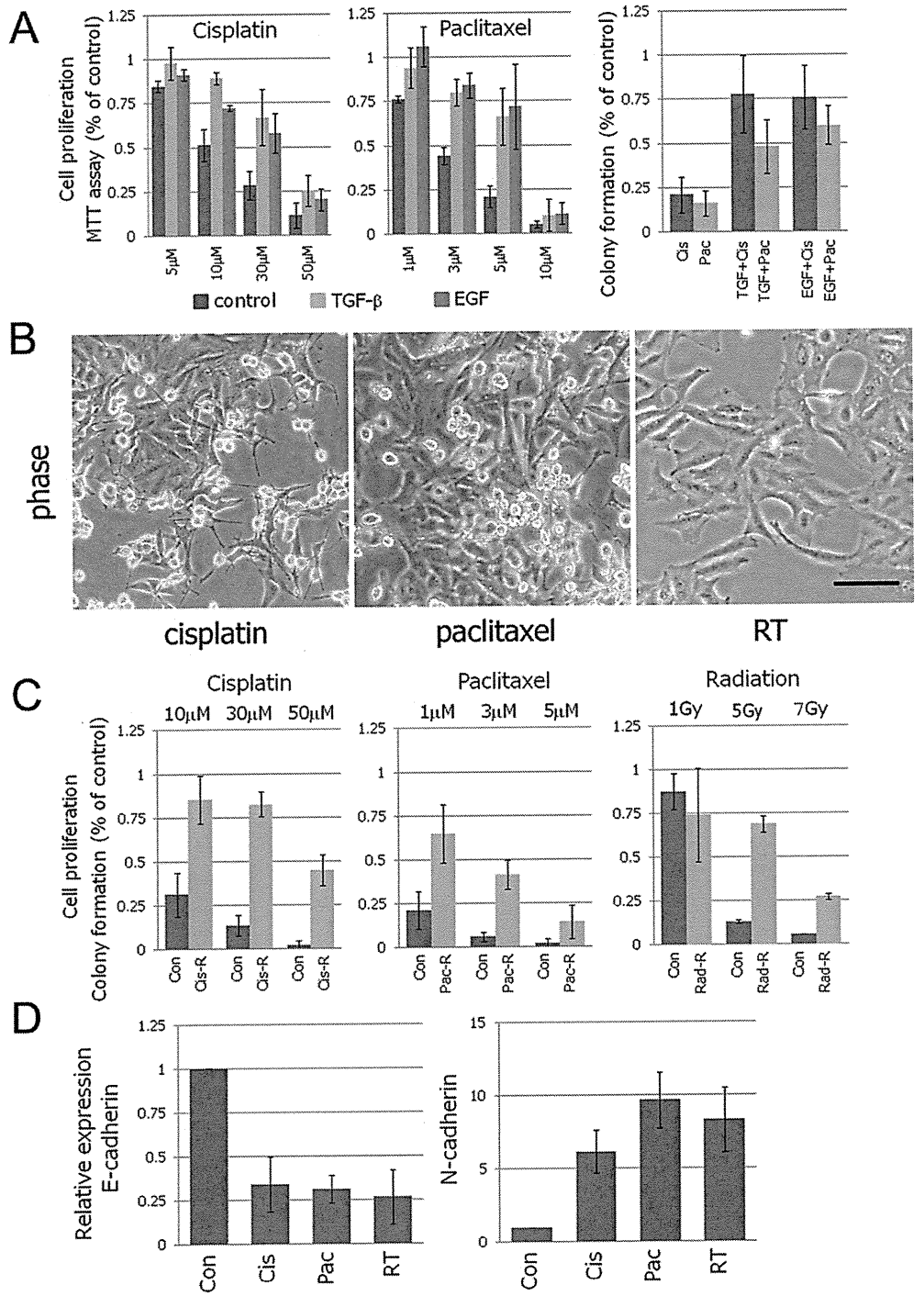

Fig 2. (A) The A549 cells were treated with cisplatin or paclitaxel after inducing EMT using TGF-β (2 ng/mL) or EGF (100 ng/mL). Proliferation of cells was quantified with MTT and clonogenic assays as described in the Material and Methods section; Cis, cisplatin (30 μM); Pac, paclitaxel (5 μM). The EMT-induced cells showed a significant increase in cell viability in response to cisplatin or paclitaxel. (B) Stable treatment-resistant phenotypes were generated by chronic exposure of A549 cells to cisplatin, paclitaxel, and radiation as described in the protocol noted in Materials and Methods section. Phase contrast images were obtained using a 4.2× objective lens. Bar = 100 μm. (C) Proliferation of resistant sub-lines was quantified with a clonogenic assay. (Con = untreated; Cis-R = cisplatin resistant; Pac-R = paclitaxel resistant; Rad-R = radiation-resistant sub-lines). Stable treatment-resistant phenotypes showed improved clonogenic survival in each resistant sub-line. (D) Total RNA was extracted from each resistant sub-line (Con = untreated; Cis = cisplatin resistant; Pac = paclitaxel resistant; RT, = radiation resistant), and real-time polymerase chain reaction was performed for E-cadherin, N-cadherin, and GAPDH (glyceraldehyde-3-phosphate dehydrogenase; as an internal control). (EMT = epithelial to mesenchymal transition; TGF = transforming growth factor.)

Ann Thorac Surg
2011;92:1794–1804

Table 1. The IC_{50} Values (Relative Resistance Ratio) for Cell Lines Against Ciplatin and Paclitaxel[a]

Cell Lines	Cisplatin (μM)	Paclitaxel (μM)
Parent A549 cells	33.2	2.9
A549 treated with TGF-β	62.8 (1.9)	5.8 (2.0)
A549 treated with EGF	55.0 (1.7)	5.5 (1.9)
Cisplatin-resistant cells	142 (4.3)	
Paclitaxel-resistant cells	22.1 (7.6)	

[a] Drug sensitivity was determined by MTT assay as described in Material and Methods. The relative resistance ratio was defined as IC_{50} of the resistant sub-line/IC_{50} of the parent cell line.

EGF = epidermal growth factor; IC_{50} = inhibitory concentration at 50%; TGF-β = transforming growth factor-beta.

cells (Fig 2A). Clonogenic assay also showed that TGF-β and EGF induced-EMT improved clonogenic survival in A549 cells (Fig 2A). Table 1 shows the IC_{50} values for cisplatin and paclitaxel in A549 cells with or without EMT induction.

EMT-Induced Cells Observed In Vitro After Exposure to Chemotherapy or Radiotherapy

A stable treatment-resistant phenotype was generated by chronic exposure of A549 cells to cisplatin, paclitaxel, or radiation. These sub-lines showed phenotypic changes such as a spindle-cell shape (Fig 2B). Table 1 shows the IC_{50} values for cisplatin and paclitaxel in parent A549 cells and drug resistance cells calculated by MTT assay. A proliferation assay showed improved clonogenic survival in each resistant sub-line (Fig 2C). The RT-PCR analysis also showed that the messenger (m)RNA level of E-cadherin was decreased, while the N-cadherin and vimentin mRNA levels were increased in the resistant cells (Fig 2D), indicating that acquisition of resistance to chemotherapy or radiation-induced molecular changes that were consistent with those induced by EMT.

Expression of EMT Markers in Clinical Samples

The characteristics of the 63 patients are shown in Table 2. Immunohistochemical staining was used to analyze the protein expressions of the epithelial markers E-cadherin and cytokeratin, and the mesenchymal markers N-cadherin and vimentin in tumor specimens. Representative immunohistochemical staining findings are shown in Figure 3. The epithelial markers were detected in nearly all biopsy specimens from patients with NSCLC before CRT whereas the mesenchymal markers were detected in 20 of 63 tumors. Tumors obtained from 13 of 63 patients showed complete response to induction CRT. While the tumor response to CRT was not significantly associated with the expression of mesenchymal markers, only 2 of the 13 tumors that achieved a complete response to CRT expressed mesenchymal proteins (Appendix 2). There was no difference in regard to DFS between patients with and without mesenchymal protein expression noted in specimens obtained before treatment (Fig 4A).

Given the results of the in vitro study, we hypothesized that preoperative CRT might induce EMT changes in tumor tissue and that these changes might be associated with a chemoresistance mechanism and poor prognosis. Thus, we compared protein expressions of the epithelial and mesenchymal markers in tumor specimens obtained both before and after CRT from patients with NSCLC. We excluded patients in whom the tumor was completely diminished after induction CRT and focused on the 50 remaining patients who showed an incomplete response to induction CRT (Table 3). While the mesenchymal

Table 2. Patient Characteristics (n = 63)

Characteristics	No. of Patients
Age	58 ± 10
Gender	
Male	56
Female	7
Clinical T status	
T1	2
T2	29
T3	17
T4	15
Clinical N status	
N0	6
N1	14
N2	41
N	32
Clinical stage	
2B	16
3A	31
3B	16
Histology	
Adenocarcinoma	27
Squamous cell carcinoma	30
Others	6
Pathologic stage	
0	13
1A–1B	16
2A–2B	12
3A	19
3B	3
Chemotherapy	
CDDP+VDS (+MMC)	38
CDDP+VNR	16
CDDP+Doce	9
Radiation (Gy)	43 ± 9.3
Surgical procedure	
Lobectomy	40
Pneumonectomy	23
With combined resection	
Bronchoplasty	8
Rib	5
Pericardium	4
Major vesse	12
Diaphragma	1

CDDP = cisplatin; Doce = docetaxel; MMC = mitomycin; VDS = vindesine; VNR = vinorelbine.

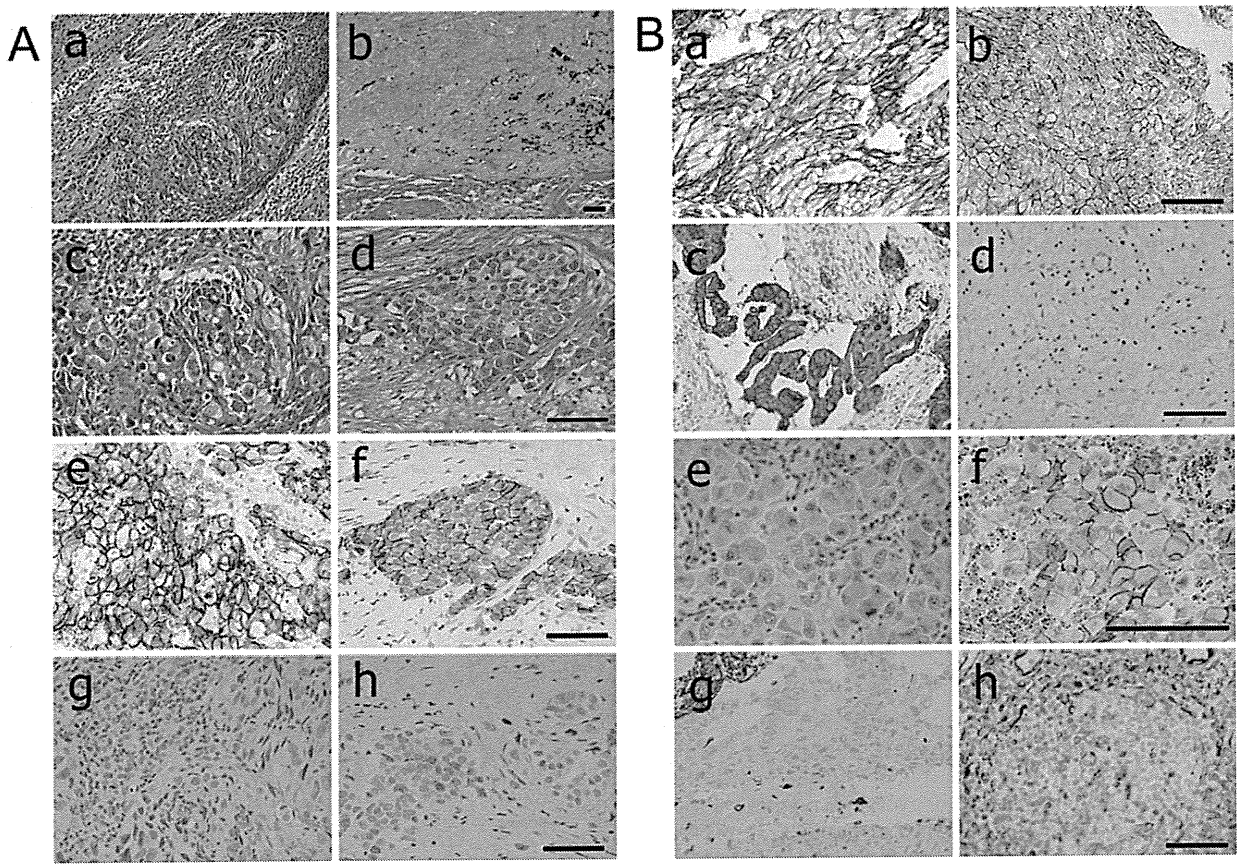

Fig 3. Immunohistochemical staining was used to analyze the protein expressions of E-cadherin and cytokeratin as epithelial markers and of N-cadherin and vimentin as mesenchymal markers in tumors before and after chemoradiotherapy (CRT) treatment. All sections were scored in a semiquantitative manner as described in the protocol noted in Materials and Methods and the staining grade was classified as 0 (score < 10), +1 (10≤, <30), +2 (30≤, <70), or +3 (70≤). (A) Panels a–h show representative findings from a patient who received induction CRT followed by surgery. a–d: hematoxylin & eosin staining; e, f: E-cadherin staining; g, h: N-cadherin staining; a, c, e, g: pre-CRT; b, d, f, h: post-CRT. (B) a, b: E-cadherin staining; c, d: cytokeratin staining, e, f: N-cadherin staining; g, h: vimentin staining; a, c, e, g: pre- CRT; b, d, f, h: post- CRT. Scale bar = 50 μm.

markers were detected in 21 of 50 tumors resected after CRT, these markers did not predict the DFS in patients with NSCLC (Fig 4B, $p = 0.239$). After CRT, expression of the epithelial markers was decreased in 15 of 50 surgically resected specimens (Table 4; Appendix 3). On the other hand, expression of the mesenchymal markers was increased after CRT in 15. In 10 of the specimens a decrease in epithelial markers and an increase in mesenchymal markers were detected, while at least one of these changes was detected in 10 specimens. Thus, a total of 20 specimens showed EMT-like changes in response to induction CRT. We classified patients with decreased epithelial markers or increased mesenchymal markers as the EMT marker-positive group (n = 20), and the others as the EMT negative group. According to a clinicopathologic comparison of these groups, the pathologic N status in the EMT marker-positive group was significantly lower than that in the EMT marker-negative group (Table 3). However, the DFS rate of patients in the EMT marker-positive group was significantly lower than that of patients in the EMT marker-negative group (Fig 4C). Five variables, including tumor response to CRT, pathologic nodal metastasis, operating procedure, histology, and EMT change, were analyzed using a Cox proportional hazards regression model to determine the variables having an effect on DFS in NSCLC patients. The univariate analyses revealed that tumor response to CRT and EMT change after CRT were related to DFS (Table 5). The multivariate analysis revealed that EMT change was an independent variable predicting DFS (Table 6).

Comment

We found that EMT leads to reduced sensitivity to chemotherapy in NSCLC cells, and that chronic exposure to chemotherapy or radiation transforms NSCLC cells into therapy-resistant sub-lines. Zhuo and colleagues [16, 17] reported that blocking EMT by knockdown of Snail or Twist, zinc finger transcription factors and key E-cadherin repressor molecules in the process of EMT,

Ann Thorac Surg
2011;92:1794–1804

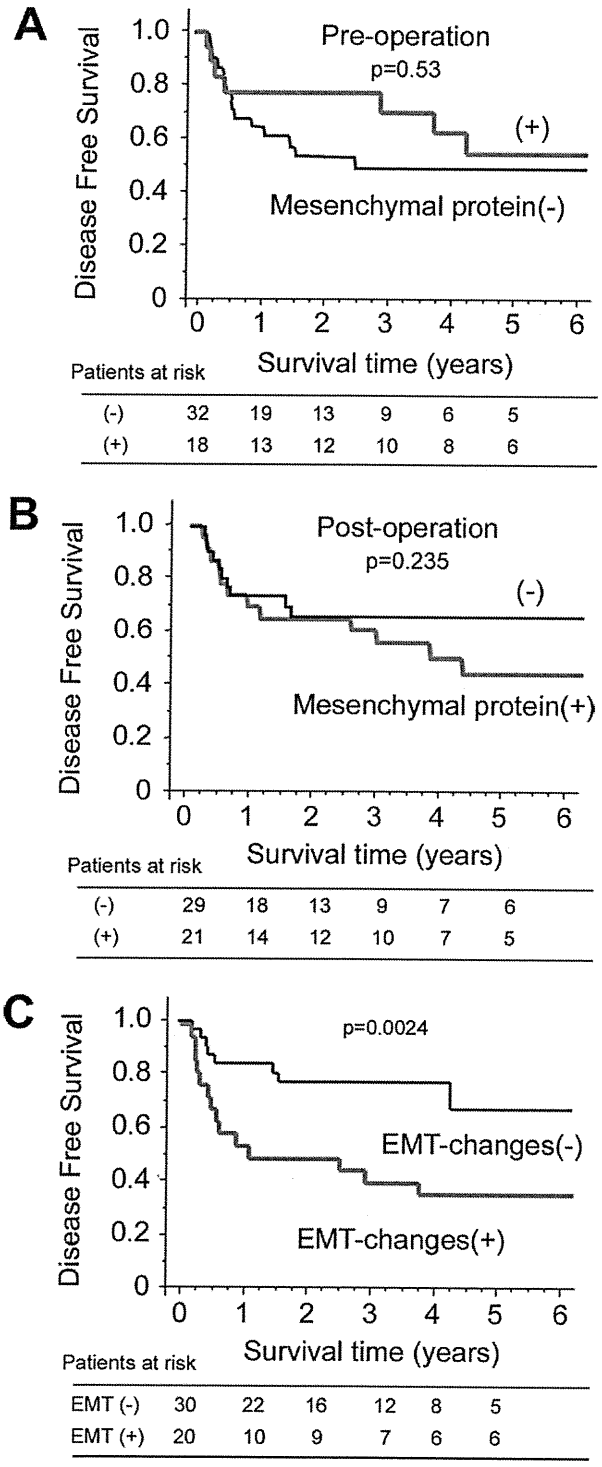

Fig 4. (A) Disease-free survival (DFS) rates according to tumor expression of mesenchymal markers before chemoradiotherapy (CRT). (B) The DFS rates according to tumor expression of mesenchymal markers after CRT. (C) The DFS rates according to EMT changes in response to CRT. The DFS rate of patients with epithelial to mesenchymal transition (EMT) changes such as decreased epithelial markers and increased mesenchymal markers as response to CRT was significantly lower than that of patients without EMT changes.

Table 3. Patient Characteristics (n = 50)

Variables	EMT-Changes After Chemoradiotherapy		
	EMT (−) (n = 30)	EMT (+) (n = 20)	*p* Value[a]
Age	59 ± 10	54 ± 10	0.039
Gender			
Male	26 (67%)	19 (95%)	0.336
Female	4 (13%)	1 (5%)	
Clinical T status			
1	0 (0%)	2 (10%)	
2	17 (57%)	8 (40%)	0.112
3	9 (30%)	4 (20%)	
4	4 (13%)	6 (30%)	
Clinical N status			
0	2 (7%)	3 (15%)	
1	7 (23%)	4 (20%)	0.787
2	20 (67%)	12 (60%)	
3	1 (3%)	1 (5%)	
Clinical stage			
2B	7 (23%)	5 (25%)	
3A	19 (63%)	8 (40%)	0.151
3B	4 (13%)	7 (35%)	
Histology			
Adenocarcinoma	11 (37%)	9 (45%)	
Squamous cell carcinoma	15 (50%)	10 (50%)	0.594
Others	4 (13%)	1 (5%)	
Chemotherapy			
CDDP+VDS (+MMC)	21 (70%)	13 (65%)	
CDDP+VNR	6 (20%)	3 (15%)	0.586
CDDP+Doce	3 (10%)	4 (20%)	
Radiation (Gy)	42 ± 10	45 ± 9.3	0.489
Surgical procedure			
Lobectomy	18 (60%)	12 (60%)	>0.999
Pneumonectomy	12 (40%)	8 (40%)	
Response to chemoradiotherapy			
Minor response	10 (33%)	4 (20%)	0.304
Major response	20 (67%)	16 (80%)	
Pathologic N status			
N0–1	16 (53%)	17 (85%)	0.021
N2	14 (47%)	3 (15%)	
Pathologic stage			
1A–1B	10 (33%)	9 (45%)	
2A–2B	5 (17%)	6 (30%)	0.195
3A–3B	15 (50%)	5 (25%)	

[a] $p = \chi^2$ test, or Mann-Whitney test.

CDDP = cisplatin; Doce = docetaxel; EMT = epithelial to mesenchymal transition; MMC = mitomycin; Response to chemoradiotherapy: Minor = more than two thirds cancer cells viable; Major = fewer than one third of cancer cells viable; VDS = vindesine; VNR = vinorelbine.

Table 4. Summary of Epithelial to Mesenchymal Transition (EMT) Status by Immunohistochemistry

EMT Markers	No. of Patients
Decrease of epithelial marker	15
E-cadherin (decrease)	14
Cytokeratin (decrease)	7
Increase mesenchymal marker	15
N-cadherin (increase)	11
Vimentin (increase)	8

increases the sensitivity of A549 cells to cisplatin. Those findings indicated that EMT is associated with acquired resistance to chemotherapy or radiotherapy in NSCLC. Furthermore, it has been reported that EMT negatively affects cellular response to EGFR-TKI (EGF receptor tyrosine kinase inhibitor) in vitro and in vivo [18]. In addition, EMT derived from repeated exposure to gefitinib, an EGFR-TKI, determines subsequent sensitivity to EGFR inhibitors as well as other anti-cancer drugs in A549 cells [23]. These data raise the possibility that an appropriate combination of CRT in an EMT-targeted strategy might be a promising approach for NSCLC therapy. Indeed, blocking EMT by restoration of E-cadherin has been shown to enhance the sensitivity to EGFR-TKI [24].

The concept of "cadherin switching" has been reported to be one of the key events in EMT in some kinds of cancer [8, 25]. Inactivation of E-cadherin is an important event in tumor progression [26, 27]. Activation of an inappropriate cadherin, such as N-cadherin, would be a subsequent event and might promote angiogenesis, brain metastasis, and poor survival [28, 29]. Basic studies have revealed interactions between N-cadherin and fibroblast growth factor receptor [30], which activates PI3K pathway signaling. Furthermore, we previously reported that stimulation of tumor stroma components induces EMT through a PI3K-extracellular signal-regulated kinases pathway [20].

Table 5. Univariate Analysis of Disease-Free Survival

Factors	Hazard Ratio	95% CI	*p* Value
Response to chemoradiotherapy			
Major versus minor	3.46	1.012–12.17	0.049
Nodal status			
pN2 vs pN0-1	1.27	0.53–3.00	0.594
Histology			
AD versus others	0.97	0.42–2.26	0.949
Surgical procedure			
Pneu versus lobe	1.10	0.47–2.57	0.831
EMT status			
EMT (+) vs (−)	3.15	1.33–7.47	0.0091

AD = adenocarcinoma; CI = confidence interval; EMT = epithelial to mesenchymal transition; lobe = lobectomy; Response to chemoradiotherapy: Minor = more than two thirds cancer cells viable; Major = fewer than one third of cancer cells viable; Pneu = pneumonectomy.

Table 6. Multivariate Analysis of Disease-Free Survival

Factors	Hazard Ratio	95% CI	*p* Value
Response to chemoradiotherapy			
Major vs minor	2.86	0.81–10.0	0.102
EMT status			
EMT (+) vs (−)	2.79	1.17–6.67	0.021

CI = confidence interval; EMT = epithelial to mesenchymal transition; Response to chemoradiotherapy: Minor = more than two thirds cancer cells viable; Major = fewer than one third of cancer cells viable.

These data suggested that survival signals in the EMT process might make cancer cells insensitive to chemoradiotherapy.

The immunohistochemistry study detected expression of mesenchymal proteins in specimens obtained from 20 of 63 patients who underwent preoperative CRT, indicating that some tumors might undergo EMT prior to treatment. Where the response to CRT was not significantly associated with the expression of mesenchymal proteins in the present study ($p = 0.067$), 2 of 12 tumors that achieved complete response to CRT expressed mesenchymal proteins, indicating that mesenchymal proteins could be biomarkers predicting response to induction CRT using biopsy specimens before treatment. In the in vitro study we investigated whether preoperative CRT might induce EMT changes in tumor tissues. A detailed study of the EMT status of NSCLC using matched specimens from both pretreatment and post-treatment is essential to investigate the association between EMT and resistance to chemotherapy or radiotherapy in patients with NSCLC. In this study we found that 20 specimens showed EMT-like changes in response to induction CRT. While the pathologic N status in the EMT marker-positive group was significantly lower than that in the EMT marker-negative group, the DFS rate of patients in the EMT marker-positive group was significantly lower than that of patients in the EMT marker-negative group. Furthermore, a Cox proportional hazards regression model revealed that the EMT-like change was an independent prognostic indicator of DFS. Thus, the changes in EMT markers induced in tumor specimens after CRT may be useful biomarkers in patients with NSCLC. We believe that the EMT change precisely indicates the malignant potential of NSCLC even in patients with down-staged disease.

In conclusion, EMT was shown to lead not only to increased malignancy potential, but also to reduced sensitivity to cisplatin, paclitaxel, and radiation in NSCLC cells. Chronic exposure to cisplatin, paclitaxel, or radiation altered NSCLC cells into therapy-resistant sub-lines. Furthermore, EMT marker expression was detected after CRT in tumors resected from patients with NSCLC. Thus, EMT may make NSCLC tumors insensitive to CRT. New therapeutic combinations using EMT-signaling inhibitors are expected to circumvent the resistance of cancers to CRT.

This work was supported by KAKENHI (Grants-in-Aid for Scientific Research) 22890106 and the Takeda Science Foundation.

References

1. Spira A, Ettinger DS. Multidisciplinary management of lung cancer. N Engl J Med 2004;350:379–92.
2. Carney DN. Lung cancer--time to move on from chemotherapy. N Engl J Med 2002;346:126–8.
3. Friedel G, Budach W, Dippon J, et al. Phase II trial of a trimodality regimen for stage III non-small-cell lung cancer using chemotherapy as induction treatment with concurrent hyperfractionated chemoradiation with carboplatin and paclitaxel followed by subsequent resection: a single-center study. J Clin Oncol 2010;28:942–8.
4. Weder W, Collaud S, Eberhardt WE, et al. Pneumonectomy is a valuable treatment option after neoadjuvant therapy for stage III non-small-cell lung cancer. J Thorac Cardiovasc Surg 2010;139:1424–30.
5. Bremnes RM, Veve R, Gabrielson E, et al. High-throughput tissue microarray analysis used to evaluate biology and prognostic significance of the E-cadherin pathway in non-small-cell lung cancer. J Clin Oncol 2002;20:2417–28.
6. Thiery JP. Epithelial-mesenchymal transitions in development and pathologies. Curr Opin Cell Biol 2003;15:740–6.
7. Wheelock MJ, Johnson KR. Cadherins as modulators of cellular phenotype. Annu Rev Cell Dev Biol 2003;19:207–35.
8. Wheelock MJ, Shintani Y, Maeda M, Fukumoto Y, Johnson KR. Cadherin switching. J Cell Sci. 2008;121(Pt 6):727–35.
9. Takeichi M. Cadherin cell adhesion receptors as a morphogenetic regulator. Science 1991;251:1451–5.
10. Liu D, Huang C, Kameyama K, et al. E-cadherin expression associated with differentiation and prognosis in patients with non-small cell lung cancer. Ann Thorac Surg 2001;71:949–54.
11. Nieman MT, Prudoff RS, Johnson KR, Wheelock MJ. N-cadherin promotes motility in human breast cancer cells regardless of their e-cadherin expression. J Cell Biol 1999;147:631–44.
12. Maeda M, Johnson KR, Wheelock MJ. Cadherin switching: Essential for behavioral but not morphological changes during an epithelium-to-mesenchyme transition. J Cell Sci 2005;118(Pt 5):873–87.
13. Bremnes RM, Veve R, Gabrielson E, et al. High-throughput tissue microarray analysis used to evaluate biology and prognostic significance of the E-cadherin pathway in non-small-cell lung cancer. J Clin Oncol 2002;20:2417–28.
14. Deeb G, Wang J, Ramnath N, et al. Altered E-cadherin and epidermal growth factor receptor expressions are associated with patient survival in lung cancer: a study utilizing high-density tissue microarray and immunohistochemistry. Mod Pathol 2004;17:430–9.
15. Soltermann A, Tischler V, Arbogast S, et al. Prognostic significance of epithelial-mesenchymal and mesenchymal-epithelial transition protein expression in non-small cell lung cancer. Clin Cancer Res 2008;14:7430–7.
16. Zhuo WL, Wang Y, Zhuo XL, Zhang YS, Chen ZT. Short interfering RNA directed against TWIST, a novel zinc finger transcription factor, increases A549 cell sensitivity to cisplatin via MAPK/mitochondrial pathway. Biochem Biophys Res Commun 2008;369:1098–102.
17. Zhuo W, Wang Y, Zhuo X, Zhang Y, Ao X, Chen Z. Knockdown of Snail, a novel zinc finger transcription factor, via RNA interference increases A549 cell sensitivity to cisplatin via JNK/mitochondrial pathway. Lung Cancer 2008;62:8–14.
18. Thomson S, Buck E, Petti F, et al. Epithelial to mesenchymal transition is a determinant of sensitivity of non-small-cell lung carcinoma cell lines and xenografts to epidermal growth factor receptor inhibition. Cancer Res 2005;65:9455–62.
19. Del Castillo G, Murillo MM, Alvarez-Barrientos A, et al. Autocrine production of TGF-beta confers resistance to apoptosis after an epithelial-mesenchymal transition process in hepatocytes: Role of EGF receptor ligands. Exp Cell Res 2006;312:2860–71.
20. Shintani Y, Maeda M, Chaika N, Johnson KR, Wheelock MJ. Collagen I promotes epithelial-to-mesenchymal transition in lung cancer cells via transforming growth factor-beta signaling. Am J Respir Cell Mol Biol 2008;38:95–104.
21. Bertolini G, Roz L, Perego P, et al. Highly tumorigenic lung cancer CD133+ cells display stem-like features and are spared by cisplatin treatment. Proc Natl Acad Sci U S A 2009;106:16281–6.
22. McCarty KS Jr, Szabo E, Flowers JL, et al. Use of a monoclonal anti-estrogen receptor antibody in the immunohistochemical evaluation of human tumors. Cancer Res 1986;46(8 Suppl):4244s–48s.
23. Rho JK, Choi YJ, Lee JK, et al. Epithelial to mesenchymal transition derived from repeated exposure to gefitinib determines the sensitivity to EGFR inhibitors in A549, a non-small cell lung cancer cell line. Lung Cancer 2009;63:219–26.
24. Witta SE, Gemmill RM, Hirsch FR, et al. Restoring E-cadherin expression increases sensitivity to epidermal growth factor receptor inhibitors in lung cancer cell lines. Cancer Res 2006;66:944–50.
25. Cavallaro U, Schaffhauser B, Christofori G. Cadherins and the tumour progression: is it all in a switch? Cancer Lett 2002;176:123–8.
26. Nakashima T, Huang C, Liu D, et al. Neural-cadherin expression associated with angiogenesis in non-small-cell lung cancer patients. Br J Cancer 2003;88:1727–33.
27. Saad AG, Yeap BY, Thunnissen FB, et al. Immunohistochemical markers associated with brain metastases in patients with nonsmall cell lung carcinoma. Cancer 2008;113:2129–38.
28. Prudkin L, Liu DD, Ozburn NC, et al. Epithelial-to-mesenchymal transition in the development and progression of adenocarcinoma and squamous cell carcinoma of the lung. Mod Pathol. 2009;22:668–78.
29. Grinberg-Rashi H, Ofek E, Perelman M, et al. The expression of three genes in primary non-small cell lung cancer is associated with metastatic spread to the brain. Clin Cancer Res 2009;15:1755–61.
30. Suyama K, Shapiro I, Guttman M, Hazan RB. A signaling pathway leading to metastasis is controlled by N-cadherin and the FGF receptor. Cancer Cell 2002;2:301–14.

Appendix 1. List of Antibodies and Other Reagents Used in This Study

Antibodies	Clone	Company	Application
Anti-E-cadherin mouse mAb	HECD-1	Takara, Shiga, Japan	IF
Anti-E-cadherin mouse mAb	NCH-38	Dako, Carpinteria, CA	IHC
Anti-N-cadherin mouse mAb	8C11	Abcam, Cambridge, MA	IF
Anti-N-cadherin mouse mAb	6G11	Dako, Carpinteria, CA	IHC
Anti-cytokeratin mouse mAb	AE1/AE3	Dako, Carpinteria, CA	IHC
Anti-vimentin mouse mAb	V9	Sigma, St. Louis, MO	IHC
Reagents			
Cisplatin		Sigma, St. Louis, MO	
Paclitaxel		Sigma, St. Louis, MO	
EGF		Sigma, St. Louis, MO	
TGF-β1		R&D Systems, Minneapolis, MO	
TaqMan assays			
E-cadherin, Hs00170423_m1		AppliedBiosystems	
N-cadherin, Hs00169953_m1			

IF = immunofluorescence; IHC = immunohistochemistry.

Appendix 2. Preoperative EMT Status and Response to Chemoradiotherapy

Response to Chemoradiotherapy	Expression of Mesenchymal Proteins		
	EMT (−)	EMT (+)	*p* Value[a]
Complete	11	2	0.155
Non-complete	32	18	

[a] *p* value from the χ^2 test.

EMT = epithelial to mesenchymal transition.

Ann Thorac Surg
2011;92:1794–1804

Appendix 3. Expression Changes of the Epithelial Markers and Mesenchymal (EMT) Markers Before and After Chemoradiotherapy

A. Expression of E-cadherin

	Post-chemoradiotherapy			
Pre-chemoradiotherapy	0	1+	2+	3+
0	0	0	0	0
1+	1	2	0	0
2+	1	0	0	0
3+	1	5	4	36

B. Expression of cytokeratin

	Post-chemoradiotherapy			
Pre-chemoradiotherapy	0	1+	2+	3+
0	1	0	0	0
1+	0	1	0	0
2+	0	1	0	1
3+	1	2	3	40

C. Expression of N-cadherin

	Post-chemoradiotherapy			
Pre-chemoradiotherapy	0	1+	2+	3+
0	33	8	0	0
1+	1	4	3	0
2+	0	0	0	0
3+	1	0	0	0

D. Expression of vimentin

	Post-chemoradiotherapy			
Pre-chemoradiotherapy	0	1+	2+	3+
0	33	3	0	0
1+	0	4	4	0
2+	0	1	1	1
3+	1	0	0	3

Changes in EMT status are indicated in bold.

DISCUSSION

DR ROSS M. BREMNER (Phoenix, AZ): You concentrate a lot on just the cancer cells themselves and the EMT [epithelial to mesenchymal transition] of the cancer cells. Can you give us your thoughts on what EMT from the stroma might be playing a role in this pre- and post-chemoradiation?

DR SHINTANI: We can see massive fibrotic area after induction chemotherapy. And as you said, we found many fibroblasts in the stroma tissues, but we did not see the EMT markers for the stroma cells. But now we have focused on the cancer associated with fibroblasts because these fibroblasts are producing many growth factors. So these fibroblasts may be the target of the cancer therapy in the future.

DR BREMNER: Thank you.

DR ALYKHAN S. NAGJI (Charlottesville, VA): The cell line that you used was an adenocarcinoma cell line. Did you find anything in the squamous cell lines, and what were the histologies of the tissues that you used?

DR SHINTANI: Your question is whether we used other cells, such as squamous cells?

DR NAGJI: Other cell lines, squamous cell. And then the histology of the tissue samples that you used, were those adenocarcinoma or squamous cell carcinoma?

DR SHINTANI: Yes. We showed only adenocarcinoma cell lines, but we used another large cell carcinoma or the squamous cell carcinoma cells.

And the last part of my talk is using human tissues and we can also see these EMT changes in the squamous cell carcinoma after induction chemoradiotherapy.

Oncogene (2011) 30, 3489–3501

www.nature.com/onc

ORIGINAL ARTICLE

MicroRNA-mediated downregulation of mTOR/FGFR3 controls tumor growth induced by Src-related oncogenic pathways

C Oneyama[1], J Ikeda[2], D Okuzaki[3], K Suzuki[1], T Kanou[1,4], Y Shintani[4], E Morii[2], M Okumura[4], K Aozasa[2] and M Okada[1]

[1]*Department of Oncogene Research, Research Institute for Microbial Diseases, Osaka University, Suita, Osaka, Japan;* [2]*Department of Pathology, Graduate School of Medicine, Osaka University, Suita, Osaka, Japan;* [3]*DNA-chip Developmental Center for Infectious Diseases, Research Institute for Microbial Diseases, Osaka University, Suita, Osaka, Japan and* [4]*Department of General Thoracic Surgery, Graduate School of Medicine, Osaka University, Suita, Osaka, Japan*

The tyrosine kinase c-Src is upregulated in various human cancers, but the molecular mechanisms underlying c-Src-mediated tumor growth remain unclear. Here we examined the involvement of microRNAs in the c-Src-mediated tumor growth. Microarray profiling revealed that c-Src activation downregulates a limited set of microRNAs, including miR-99a, which targets oncogenic mammalian target of rapamycin (mTOR) and fibroblast growth factor receptor 3 (FGFR3). Re-expression of miR-99a suppressed tumor growth of c-Src-transformed cells, and this effect was restored by the overexpression of mTOR. The downregulation of miR-99a was also observed in epidermal growth factor- and Ras-transformed cells, and it was suppressed by inhibiting the mitogen-activated protein kinase (MAPK) pathway. Furthermore, miR-99a downregulation is associated with mTOR/FGFR3 upregulation in various human lung cancer cells/tissues. The tumorigenicity of these cells was suppressed by the introduction of miR-99a. These findings suggest that the miR-99a-mTOR/FGFR3 pathway is crucial for controlling tumor growth in a wide range of human cancers that harbor upregulation of the Src-related oncogenic pathways.
Oncogene (2011) **30,** 3489–3501; doi:10.1038/onc.2011.63; published online 7 March 2011

Keywords: c-Src; tumor; miRNA; mTOR; FGFR3

Introduction

The tyrosine kinase c-Src is a pivotal component of multiple signaling pathways that regulate cell proliferation, survival, adhesion and migration, which are processes tightly associated with tumor progression (Brown and Cooper, 1996; Ingley, 2008). c-Src is frequently overexpressed and activated in a wide variety of human cancers, suggesting a role in tumor progression (Frame, 2002; Ishizawar and Parsons, 2004; Yeatman, 2004). In normal cells, the kinase activity of c-Src is rigorously controlled by the C-terminal Src kinase (Csk) (Nada *et al.*, 1991; Okada *et al.*, 1991); therefore, the oncogenic potential of c-Src is suppressed even when c-Src is abundantly expressed. In some cancer cells, however, c-Src function is upregulated despite the fact that the *c-src* gene is rarely mutated (Irby *et al.*, 1999; Irby and Yeatman, 2000). Thus, it is considered that disruption of the strict regulation of c-Src may trigger cancer progression, although the underlying mechanisms remain unclear. Once activated, c-Src acts as a common upstream regulator of various oncogenic pathways, including the Ras/MAPK pathway, STAT and phosphoinositide 3-kinase (PI3K) pathways (Ingley, 2008), to induce the phenotypic changes characteristic of cell transformation. Mounting evidence shows the importance of c-Src in cancer progression, but the complexity of c-Src function has hampered the elucidation of the critical c-Src pathways involved in directing tumor growth.

MicroRNAs (miRNAs) are a class of small RNA molecules approximately 22 nucleotides long that regulate gene expression by blocking mRNA translation and/or mediating mRNA degradation (Ambros, 2004; Bartel, 2004, 2009; Ventura and Jacks, 2009). More than 600 different miRNAs have so far been identified in human beings, and they have been shown to control diverse cellular functions, including cell proliferation and differentiation (He and Hannon, 2004; Bartel, 2009). Each miRNA is predicted to target hundreds of genes, and each transcript may interact with multiple miRNAs (Bartel, 2009). This interplay between miRNA and transcripts underscores the potential role of miRNAs as key regulators of complex signaling networks. In recent years, numerous studies have shown aberrant expression of miRNAs in human cancers (Calin and Croce, 2006; Esquela-Kerscher and Slack, 2006). In addition, some miRNAs are located in unstable genomic regions and are often downregulated in tumors (Calin and Croce, 2006). These lines of evidence strongly suggest that a group of miRNAs functions as oncogenes or tumor suppressors (Shenouda and Alahari, 2009).

Correspondence: Dr C Oneyama, Department of Oncogene Research, Research Institute for Microbial Diseases, Osaka University, 3-1 Yamadaoka, Suita, Osaka 565-0871, Japan.
E-mail: coneyama@biken.osaka-u.ac.jp
Received 3 November 2010; revised 16 January 2011; accepted 4 February 2011; published online 7 March 2011

The PI3K pathway is a key signal-transduction system that links multiple receptors and oncogenic molecules to diverse cellular functions and is inappropriately activated in many human cancers (Engelman, 2009; Liu *et al.*, 2009). Mammalian target of rapamycin (mTOR) is a serine–threonine kinase that is a major downstream effector of the PI3K pathway and plays a crucial part in the regulation of cell growth by monitoring nutrient availability, cellular energy levels, oxygen levels and mitogenic signals (Wullschleger *et al.*, 2006). The mTOR signaling pathway has also been implicated in tumorigenesis (Petroulakis *et al.*, 2006; Guertin and Sabatini, 2007; Nagaraja *et al.*, 2010). Indeed, rapamycin, a selective mTORC1 inhibitor, has antineoplastic properties, and its analogues have been developed as anticancer drugs. Major downstream targets of mTORC1 are ribosomal protein S6 kinase 1 (S6K1, also known as p70S6K) and eukaryotic translation initiation factor 4E-binding protein 1, both of which play crucial roles in the regulation of protein synthesis (Hay and Sonenberg, 2004). Therefore, activation of the mTOR pathway provides tumor cells with a growth advantage by promoting protein synthesis (Sabatini, 2006; Menon and Manning, 2008). In human cancers, the PI3K pathway is activated by either upregulation of receptor tyrosine kinases or somatic mutations in specific components of the pathway (Liu *et al.*, 2009). Fibroblast growth factor receptor 3 (FGFR3) is one of the receptors that promote cell survival by stimulating PI3K-AKT signaling (Ong *et al.*, 2001). Overexpression and/or mutation of FGFR3 are frequently observed in myeloma, ovarian and bladder cancers, suggesting that this molecule plays a role in tumorigenesis (van Rhijn *et al.*, 2001; Eswarakumar *et al.*, 2005).

To address the molecular mechanisms underlying c-Src-mediated cell transformation, we previously developed a model system using Csk-deficient fibroblasts ($Csk^{-/-}$ cells) that can be transformed by wild-type c-Src (Oneyama *et al.*, 2008). In this system, the activation of relatively small numbers of molecules is sufficient for induction of cell transformation and tumorigenesis (Oneyama *et al.*, 2008). These findings suggest that this system could be useful in the identification of critical pathways leading to c-Src transformation. In this study, this experimental system was applied for the analysis of potential contribution of miRNAs to c-Src-mediated tumor growth. Expression profiling of miRNAs in $Csk^{-/-}$ cells revealed that a limited set of miRNAs are differentially regulated by c-Src transformation. In particular, we focused our analysis on miR-99a based on its significant downregulation by c-Src transformation. We show that miR-99a is downregulated in various human cancers and targets *mTOR* and *FGFR3* genes that are tightly associated with human cancers. Functional analysis of miR-99a in c-Src/Ras-transformed cells and various human cancer cells/tissues suggests that miR-99a is downregulated by the activation of Src-related oncogenic pathways and functions as a suppressor of tumor growth by controlling the expression of mTOR/FGFR3.

Results

miRNA expression profiling in c-Src-transformed cells

Previously, we developed an experimental system using $Csk^{-/-}$ cells to analyze the molecular mechanisms underlying c-Src-mediated transformation (Oneyama *et al.*, 2008). Despite the activation of endogenous c-Src, the cells do not transform owing to the substantial degradation of activated c-Src by the ubiquitin–proteasome system (Hakak and Martin, 1999). However, exogenous expression of c-Src, at levels over twice the endogenous level, efficiently induced cell transformation (Oneyama *et al.*, 2008). Using these cells, we compared the expression profiles of miRNAs between non-transformed cells ($Csk^{-/-}$ cells and those expressing Csk or c-Src plus Csk) and c-Src-transformed cells ($Csk^{-/-}$ cells expressing c-Src) through miRNA microarray analysis. Pair-wise significance analysis of the microarray data (see Supplementary information) indicated that seven *miRNA* genes were downregulated (Figure 1a) and six *miRNA* genes were significantly upregulated in c-Src-transformed cells.

Quantitative real-time PCR (qRT–PCR) analyses confirmed the downregulation of the seven miRNAs in c-Src-transformed cells (Figure 1b). These miRNAs were categorized into three clusters based on their chromosomal locations of mouse: miR-23b and -27b are located on chromosome (Chr.) 13, miR-322, -450a, -503 and -542 are on Chr. X, and miR-99a is on Chr. 16. These findings suggest a potential role of these miRNAs in regulating transformation via the c-Src-mediated pathway.

miR-99a as a suppressor of c-Src-induced tumor growth

Recent studies have reported that miR-99a is transcribed from the commonly deleted region at 21q21 in human lung cancers (Nagayama *et al.*, 2007; Yamada *et al.*, 2008) and that miR-99a is downregulated in ovarian carcinoma (Nam *et al.*, 2008), squamous cell carcinoma of the tongue (Wong *et al.*, 2008), bladder cancer (Catto *et al.*, 2009), squamous cell lung carcinoma (Gao *et al.*, 2010) and childhood adrenocortical tumors (Doghman *et al.*, 2010). These findings indicate that miR-99a is widely downregulated in human cancers, suggesting a potential role for miR-99a as a tumor suppressor. Thus, we further concentrated on miR-99a and tested if miR-99a is involved in regulating c-Src-induced transformation and tumor growth. Overexpression of miR-99a did not induce changes in cell morphology or cytoskeletal organization of c-Src-transformed cells (Figure 2a). In addition, miR-99a expression did not affect c-Src-induced tyrosine phosphorylation of cellular proteins or the activity of c-Src (pY416) or Erk (p-Erk), although it slightly inhibited AKT activity (Figure 2b). An *in vitro* proliferation assay showed that miR-99a expression only weakly suppressed anchorage-dependent growth of these cells (Supplementary Figure 1). However, a colony formation assay in soft agar revealed that miR-99a expression dramatically suppressed anchorage-independent growth of c-Src-transformed cells in a dose-dependent manner

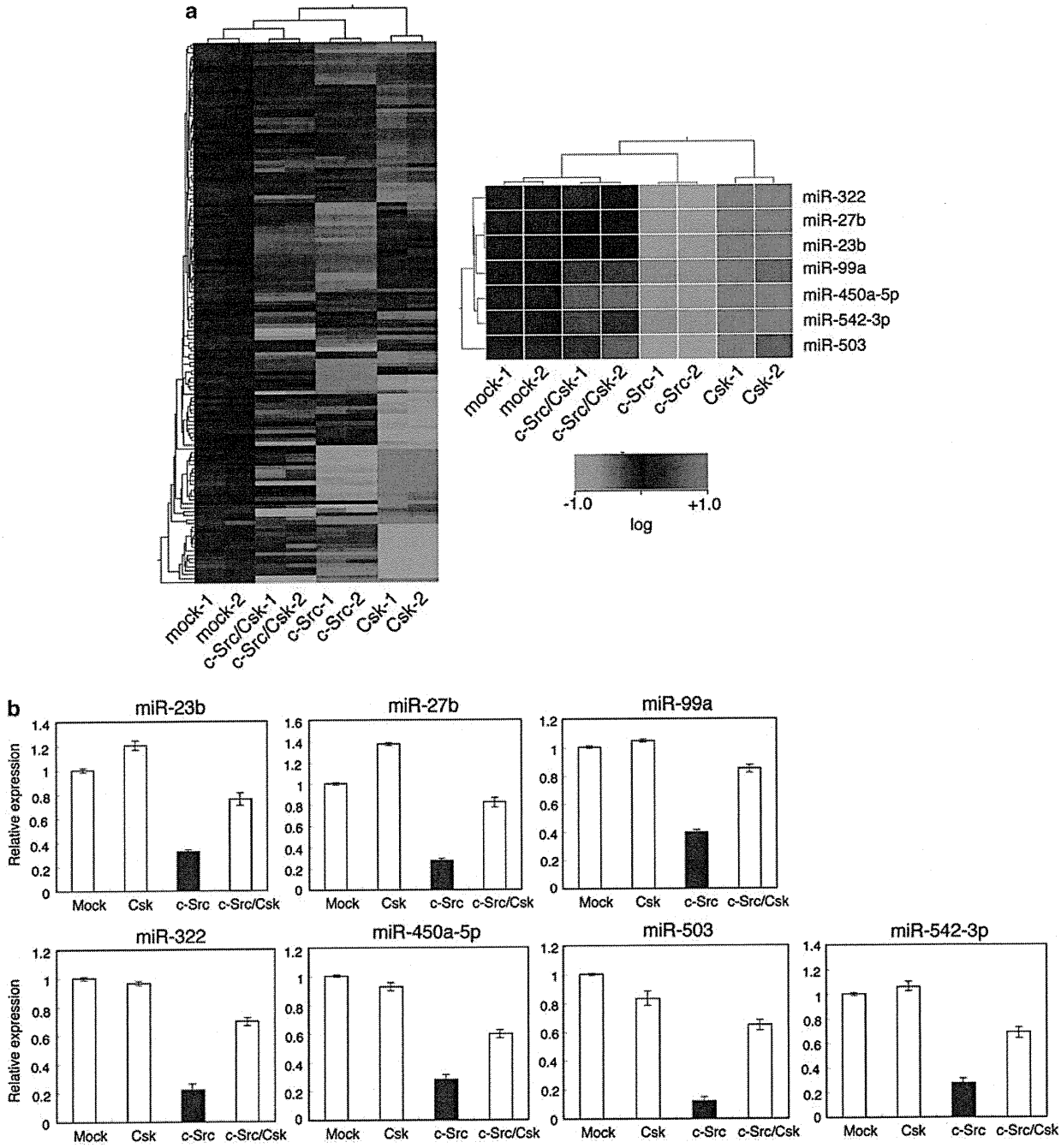

Figure 1 miRNA expression profiling in c-Src-transformed cells. (**a**) Hierarchical clustering of 138 miRNAs that exhibited significantly altered expression in c-Src/Csk-, c-Src- or Csk-expressing cells compared with mock $Csk^{-/-}$ cells is shown as described in the Supplementary information (left side). Of the 138 miRNAs, seven miRNAs (miR-322, -27b, -23b, -99a, -450a-5p, -542-3p and -503) that downregulated twofold in c-Src-transformed cells were subjected to hierarchical clustering (right side). In each panel, the selected miRNAs are shown in the lines and four pairs of duplicates in the columns. The color bar indicates the fold-change (log 2). Red denotes upregulated and green denotes downregulated. (**b**) The expression of seven miRNAs downregulated was analyzed using qRT–PCR. Relative values ± s.d. were obtained from three independent assays.

(Figure 2c). Tumorigenesis of c-Src-transformed cells in nude mice was also remarkably suppressed by the expression of miR-99a (Figure 2d). These results suggest that miR-99a functions as a suppressor of tumor growth induced by the activation of c-Src in these cells.

miR-99a targets mTOR and FGFR3

To elucidate the function of miR-99a, we performed a bioinformatic search (Targetscan and Pictar) for putative targets of miR-99a. Interestingly, miR-99a was found to have relatively few potential targets

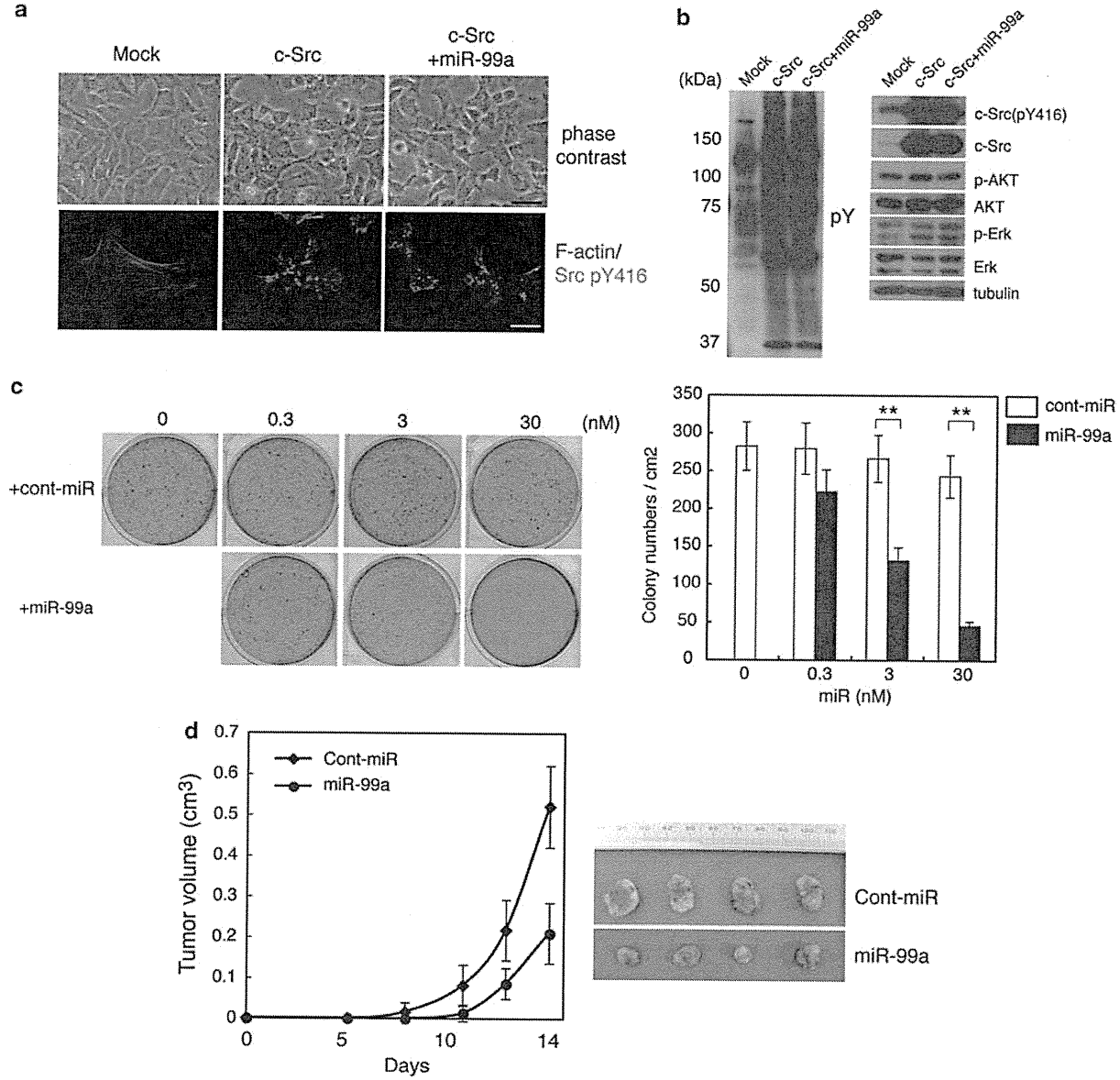

Figure 2 miR-99a as a suppresser of c-Src-induced tumor growth. (**a**) The morphology of $Csk^{-/-}$ cells expressing c-Src and miR-99a was observed under phase-contrast microscopy (upper panels). Actin filaments (red) and intracellular localization of activated Src (Src pY416: green) in the indicated cells were analyzed by immunostaining (lower panels). A white and a black scale bar represents 20 and 50 μm, respectively. (**b**) Total cell lysates from $Csk^{-/-}$ cells expressing c-Src and miR-99a were immunoblotted with the antibodies indicated. (**c**) Soft-agar colony formation assays of c-Src-transformed cells treated with 0.3–30 nM of miR-99a or control (cont-miR). Representative dishes from three independent experiments are shown (left panels). The mean number of colonies ± s.d. was obtained from three independent experiments (right panel). (**d**) The effect of miR-99a expression on tumorigenicity in nude mice. c-Src-transformed cells treated with miR-99a were inoculated subcutaneously into nude mice. Averages ± s.d. of tumor volume (cm^3) obtained from four mice are plotted vs time after inoculation (days). Excised tumors are shown in the right panels.

(around 40), which included several cell signaling molecules. Among the candidates, the 3′-untranslated regions of mTOR and FGFR3 contained regions that matched the seed sequences of miR-99a (Figure 3a). A luciferase reporter assay in c-Src-transformed cells showed that miR-99a specifically targeted the miR-99a binding sequences in mTOR and FGFR3 mRNAs (Figure 3b). Conversely, introduction of anti-miR-99a enhanced the expression of luciferase reporter of both constructs in non-transformed $Csk^{-/-}$ cells, which express miR-99a at higher levels (Figure 3c). These results indicate that miR-99a can directly target mTOR and FGFR3 mRNA to regulate their expression.

We then examined the impact of miR-99a expression on the endogenous mTOR and FGFR3 proteins. Western blot analysis showed that both proteins were upregulated by c-Src transformation (Figure 3d, lanes 1 vs 3), whereas they were significantly downregulated by